

Proceedings of the International Astronomical Union

Date of delivery: 5 May 2016

Journal and vol/article ref: IAU 1600043

Number of pages (not including this page): 6

This proof is sent to you on behalf of Cambridge University Press. Please check the proofs carefully. Make any corrections necessary on a hardcopy and answer queries on each page of the proofs

Please return the **marked proof** within **5** days of receipt to:

Managing editor of this symposium

Authors are strongly advised to read these proofs thoroughly because any errors missed may appear in the final published paper. This will be your ONLY chance to correct your proof. Once published, either online or in print, no further changes can be made.

To avoid delay from overseas, please send the proof by airmail or courier.

If you have **no corrections** to make, please email **managing editor** to save having to return your paper proof. If corrections are light, you can also send them by email, quoting both page and line number.

- The proof is sent to you for correction of typographical errors only. Revision of the substance of the text is not permitted, unless discussed with the editor of the journal. Only **one** set of corrections are permitted.
- Please answer carefully any author queries.
- Corrections which do NOT follow journal style will not be accepted.
- A new copy of a figure must be provided if correction of anything other than a typographical error introduced by the typesetter is required.

If you do not send any corrections to the editor within 5 days, we will assume your proof is acceptable.

- If you have problems with the file please contact

lwebb@cambridge.org

Please note that this pdf is for proof checking purposes only. It should not be distributed to third parties and may not represent the final published version.

Important: you must return any forms included with your proof. We cannot publish your article if you have not returned your signed copyright form.

NOTE - for further information about **Journals Production** please consult our **FAQs** at http://journals.cambridge.org/production_faqs

Author queries:

Typesetter queries:

Non-printed material:

High dispersion spectroscopy of solar-type superflare stars with Subaru/HDS †

Yuta Notsu^{1,*}, Satoshi Honda², Hiroyuki Maehara³, Shota Notsu¹,
Takuya Shibayama⁴, Daisaku Nogami¹ and Kazunari Shibata⁵

*email: ynotsu@kwasan.kyoto-u.ac.jp

¹Department of Astronomy, Kyoto University, Kitashirakawa-Oiwake-cho, Sakyo-ku, Kyoto, Japan, 606-8502

²Center for Astronomy, University of Hyogo, 407-2, Nishigaichi, Sayo-cho, Sayo, Hyogo, Japan, 679-5313

³Okayama Astrophysical Observatory, National Astronomical Observatory of Japan, 3037-5 Honjo, Kamogata, Asakuchi, Okayama, Japan, 719-0232

⁴Institute for Space-Earth Environmental Research, Nagoya University, Furo-cho, Chikusa-ku, Nagoya, Aichi, Japan, 464-8601

⁵Kwasan and Hida Observatories, Kyoto University, Yamashina-ku, Kyoto, Japan, 607-8471

Abstract. We carried out spectroscopic observations with Subaru/HDS of 50 solar-type superflare stars found from Kepler data. More than half (34 stars) of the target stars show no evidence of the binary system, and we confirmed atmospheric parameters of these stars are roughly in the range of solar-type stars.

We then conducted the detailed analyses for these 34 stars. First, the value of the “ $v \sin i$ ” (projected rotational velocity) measured from spectroscopic results is consistent with the rotational velocity estimated from the brightness variation. Second, there is a correlation between the amplitude of the brightness variation and the intensity of Ca II IR triplet line. All the targets expected to have large starspots because of their large amplitude of the brightness variation show high chromospheric activities compared with the Sun. These results support that the brightness variation of superflare stars is explained by the rotation of a star with large starspots.

Keywords. stars:activity, stars:flare, stars:rotation, stars:solar-type, stars:starspots

1. Introduction

Flares are energetic explosions in the stellar atmosphere, and are thought to occur by intense releases of magnetic energy stored around starspots, like solar flares (e.g., Shibata & Magara 2011). Superflares are flares $10\sim 10^6$ times more energetic ($\sim 10^{33-38}$ erg; Schaefer *et al.* 2000) than the largest solar flares ($\sim 10^{32}$ erg). Recently, we analyzed the data of the Kepler space telescope (Koch *et al.* 2010), and discovered more than 1000 superflares on a few hundred solar-type (G-type main-sequence) stars (Maehara *et al.* 2012, 2015; Shibayama *et al.* 2013; Candelaresi *et al.* 2014). We here define solar-type stars as the stars that have a surface temperature of $5100 \leq T_{\text{eff}} \leq 6000\text{K}$ and a surface gravity of $\log g \geq 4.0$.

With these data, we studied the statistical properties of the occurrence rate of superflares, and found that the occurrence rate (dN/dE) of the superflare versus the flare energy (E) has a power-law distribution of $dN/dE \propto E^{-\alpha}$, where $\alpha \sim 2$ (Maehara *et al.* 2012, 2015; Shibayama *et al.* 2013), and this distribution is roughly similar to that for the solar flare.

† This study is based on observational data collected with Subaru Telescope, which is operated by the National Astronomical Observatory of Japan.

Many of the superflare stars show quasi-periodic brightness variations with a typical period of from one day to a few tens of days. The amplitude of these brightness variations is in the range of 0.1-10% (Maehara *et al.* 2012), and is much larger than that of the solar brightness variation (0.01-0.1%) caused by the existence of sunspots on the rotating solar surface. Notsu *et al.* (2013b) showed that the above brightness variations of superflare stars can be well explained by the rotation of a star with fairly large starspots, taking into account the effects of inclination angle and the spot latitude.

Notsu *et al.* (2013b) compared the superflare energy and frequency with the rotation period, assuming that the brightness variation corresponds to the rotation. They then found slowly rotating stars can still produce as energetic flares as those of more rapidly rotating stars, though the average flare frequency is lower for more slowly rotating stars. Notsu *et al.* (2013b) also clarified that the superflare energy is related to the total coverage of the starspots, and that the energy of superflares can be explained by the magnetic energy stored around these large starspots. In addition, Shibata *et al.* (2013) suggested, on the basis of theoretical estimates, that the Sun can generate large magnetic flux sufficient for causing superflares with an energy of 10^{34} erg within one solar cycle.

The results described above are, however, only based on Kepler monochromatic photometric data. We need to spectroscopically investigate whether these brightness variations are explained by the rotation, and whether superflare stars have large starspots. The stellar parameters and the binarity of the superflare stars are also needed to be investigated with spectroscopic observations in order to discuss whether the Sun can really generate superflares. We have then performed high-dispersion spectroscopy of superflares stars (50 stars in total). We describe the results of this observation in the following.

2. Observations

In this observation, we observed 50 solar-type superflare stars by using High Dispersion Spectrograph (HDS; Noguchi *et al.* 2002) at the 8.2m Subaru telescope on 6 nights during 2011~2013 (Notsu *et al.* 2013a, 2015a & 2015b; Nogami *et al.* 2014; Honda *et al.* 2015). These 50 target stars were selected from superflare stars reported by our previous researches (e.g., Shibayama *et al.* 2013). Spectroscopic resolution ($R = \lambda/\Delta\lambda$) of each observation date is $R = 50,000 \sim 100,000$. The wavelength range is 6100~8800Å. This range includes Ca II near-IR triplet (8498/8542/8662Å) and H α (6563Å), which are well-known indicators of stellar chromospheric activity. More details of the observations and the target stars are described in Notsu *et al.* (2015a).

3. Results and discussion

3.1. Stellar parameters

As a result of the observations, we found more than half (34 stars) of our 50 targets have no evidence of binary system (Notsu *et al.* 2015a). Among the remaining 16 stars, 12 stars show double line profiles or radial velocity shifts, which are expected to be caused by the orbital motion of binary system. The other 4 stars have visual companion stars. We then estimated effective temperature (T_{eff}), surface gravity ($\log g$), metallicity ($[\text{Fe}/\text{H}]$), and projected rotation velocity ($v \sin i$) of these 34 “single” superflare stars on the basis of our spectroscopic data (Notsu *et al.* 2015a). We here estimated $v \sin i$ by measuring Doppler broadening of photospheric lines taking into account macroturbulence and instrumental broadening (cf. Takeda *et al.* 2008; Notsu *et al.* 2015a).

We confirmed that stellar atmospheric parameters (T_{eff} , $\log g$, and $[\text{Fe}/\text{H}]$) of the 34 target stars are roughly in the range of ordinary solar-type (G-type main sequence) stars. In particular, the temperature, surface gravity, and brightness variation period (P) of 9

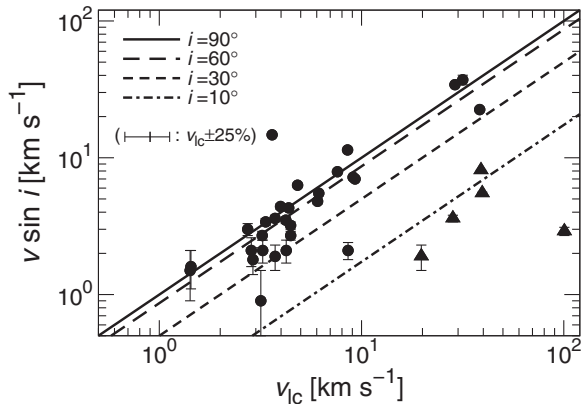


Figure 1. Projected rotational velocity ($v \sin i$) as a function of the stellar rotational velocity (v_{1c}) estimated from the period of the brightness variation and stellar radius. The typical error of v_{1c} is about $\pm 25\%$ of each value, considering errors of P and R_s (Notsu *et al.* 2015a). The solid line represents the case that our line of sight is vertical to the stellar rotation axis ($i = 90^\circ$; $v \sin i = v_{1c}$). We also plot three different lines, which correspond to smaller inclination angles ($i = 60^\circ, 30^\circ, 10^\circ$). Filled triangles represent superflare stars whose inclination angle is especially small ($i \leq 13^\circ$), while filled circles represent the other stars ($i > 13^\circ$).

stars are in the range of “Sun-like” stars ($5600 \leq T_{\text{eff}} \leq 6000\text{K}$, $\log g \geq 4.0$, and $P > 10$ days). Five of the 34 target stars are fast rotators ($v \sin i \geq 10\text{km s}^{-1}$), while 22 stars have relatively low $v \sin i$ values ($v \sin i < 5\text{km s}^{-1}$). These results suggest that stars whose spectroscopic properties similar to the Sun can have superflares, and this supports the hypothesis that the Sun might cause a superflare. In the following, we conducted the detailed analyses for these 34 single stars (Notsu *et al.* 2015b).

3.2. Rotational velocity and inclination angle

We here compare “ $v \sin i$ ” with the brightness variation period (P), and consider whether the brightness variation of superflare stars is explained by the rotation. Assuming that the brightness variations are caused by the rotation of the stars with starspots, we can estimate the rotational velocity (v_{1c}) from P and R_s (stellar radius) by using

$$v_{1c} = \frac{2\pi R_s}{P}. \quad (3.1)$$

In Figure 1, we plot $v \sin i$ as a function of the v_{1c} . Some data points in Figure 1 show differences between the values of v_{1c} and $v \sin i$. The projected rotational velocity ($v \sin i$) tends to be smaller than v_{1c} . Such differences should be explained by the inclination effect, as in Notsu *et al.* (2013a). On the basis of $v \sin i$ and v_{1c} , the stellar inclination angle (i) can be estimated by using the following relation:

$$i = \arcsin\left(\frac{v \sin i}{v_{1c}}\right). \quad (3.2)$$

In Figure 1, we also show four lines indicating $i = 90^\circ$ ($v \sin i = v_{1c}$), $i = 60^\circ$, $i = 30^\circ$, and $i = 10^\circ$. This figure shows two following important results. First, for almost all the stars (33 stars), the relation “ $v \sin i \lesssim v_{1c}$ ” is satisfied. This is consistent with our assumption that the brightness variation is caused by the rotation since the inclination effect mentioned above can cause the relation “ $v \sin i \lesssim v_{1c}$ ” if v_{1c} values really correspond to the rotational velocities (i.e. $v = v_{1c}$). This is also supported by another fact that

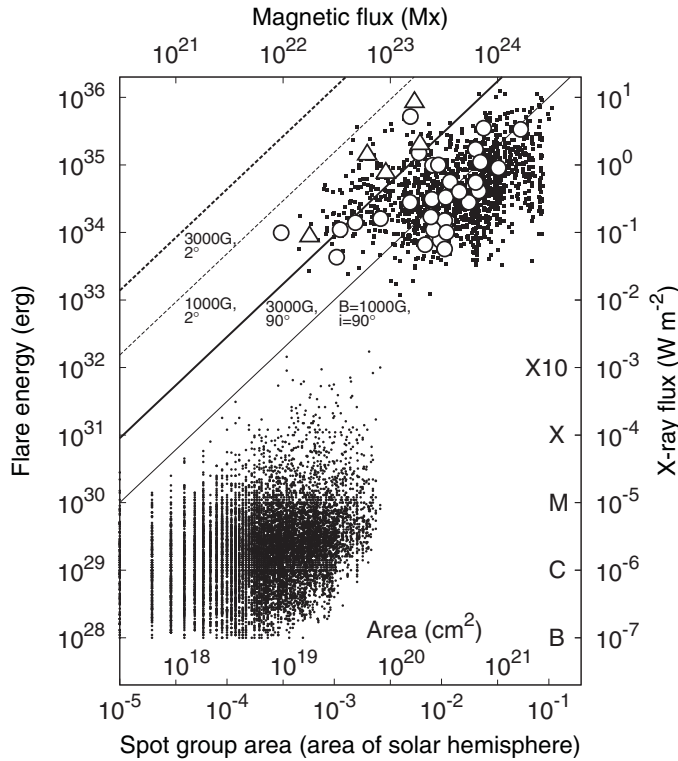


Figure 2. Scatter plot of the flare energy as a function of the spot coverage. The data of superflares on solar-type stars (filled squares) and solar flares (filled circles) in this figure are completely the same as those in Figure 10 of Notsu *et al.* (2013b). Thick and thin solid lines corresponds to the analytic relation between the spot coverage and the flare energy, which is obtained from Equation (14) of Notsu *et al.* (2013b) for $B=3,000\text{G}$ and $1,000\text{G}$. The thick and thin dashed lines correspond to the same relation in case of $i = 2^\circ$ (nearly pole-on) for $B=3,000\text{G}$ and $1,000\text{G}$. Open circle and triangle points on the filled squares represent the data points of the most energetic superflare event reported in Shibayama *et al.* (2013) of the 34 target superflare stars. Open triangles represent superflare stars whose inclination angle is especially small ($i \leq 13^\circ$), while open circles represent the others ($i > 13^\circ$). This classification is on the basis of Figure 1.

the distribution of the data points in Figure 1 are not random. Their distribution is expected to be much more random if the brightness variations have no relations with the stellar rotation. Second, stars that are distributed in the lower right side of Figure 1 are expected to have small inclination angles and to be nearly pole-on stars. In this figure, we distinguish such five stars with especially small inclination angle ($i \leq 13^\circ$) from the other stars, using filled triangle data points.

We can confirm the above inclination effects from another point of view. Figure 2 is a scatter plot of the flare energy of superflares and solar flares as a function of the spot coverage. The spot coverage of superflare stars is calculated from the amplitude of stellar brightness variations. Thick and thin solid lines correspond to the analytic relation between the spot coverage and the flare energy, which is obtained from Equation (14) of Notsu *et al.* (2013b) in case of $i = 90^\circ$ for $B=3,000\text{G}$ and $1,000\text{G}$. The thick and thin dashed lines correspond to the same relation in case of $i = 2^\circ$ (nearly pole-on) for $B=3,000\text{G}$ and $1,000\text{G}$, assuming that the brightness variation becomes small as a result of the inclination effect. These lines are considered to give an upper limit of superflare

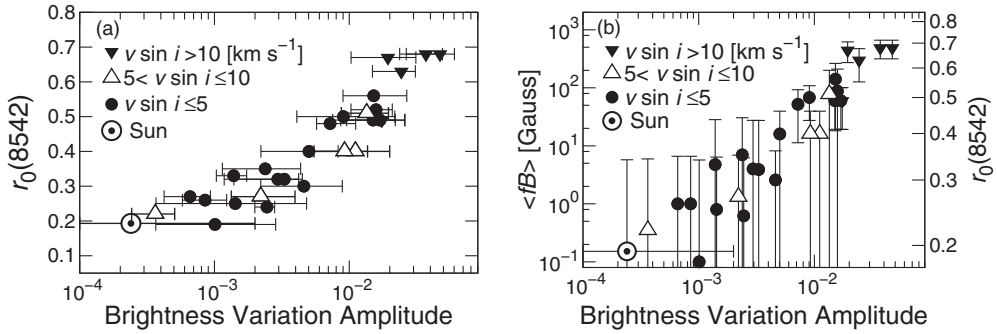


Figure 3. (a) $r_0(8542)$ as a function of the amplitude of stellar brightness variation ($\langle \text{BVamp} \rangle$). The results of the target superflare stars are plotted, being classified into three groups on the basis of $v \sin i$ (projected rotation velocity). The solar value is plotted by using a circled dot point. (b) $\langle fB \rangle$ as a function of amplitude of stellar brightness variation. $\langle fB \rangle$ values are estimated from $r_0(8542)$ on the basis of the rough relation estimated in Notsu *et al.* (2015b).

energy for each inclination angle. Considering these things, the superflare stars located in the upper left side of this figure are expected to have a low inclination angle. Open triangles in Figure 2 correspond to superflare stars whose inclination angle is especially small ($i \leq 13^\circ$) on the basis of Figure 1, while open circles represent the other stars ($i > 13^\circ$). This classification is the same as that in Figure 1. All of the five triangle data points are located above the thick solid line ($i = 90^\circ$ and $B=3000\text{G}$). This means that these stars are confirmed to have low inclination angle on the basis of both of the Figures 1 and 2. As a result, these two figures (Figures 1 and 2) are confirmed to be consistent. In other words, the stellar projected rotational velocity spectroscopically measured is consistent with the rotational velocity estimated from the brightness variation. This fact supports that the brightness variation of superflare stars is caused by the rotation.

3.3. Stellar chromospheric activity and starspots of superflare stars

In order to investigate the chromospheric activity of the target stars, we measured $r_0(8498)$, $r_0(8542)$, $r_0(8662)$, and $r_0(\text{H}\alpha)$ index, which are the residual core flux normalized by the continuum level at the line cores of the Ca II IRT and $\text{H}\alpha$, respectively. These indexes are known to be good indicators of stellar chromospheric activity (e.g., Takeda *et al.* 2010; Notsu *et al.* 2013a). As the chromospheric activity is enhanced, the intensity of these indicators becomes large since a greater amount of emission from the chromosphere fills in the core of the lines.

The $r_0(8542)$ values are plotted in Figure 3 (a) as a function of the amplitude of stellar brightness variation ($\langle \text{BVamp} \rangle$) of Kepler data. First, almost all the target superflare stars are more active compared with the Sun from the viewpoint of the $r_0(8542)$ index. In other words, the mean magnetic field strength of the target stars can be higher than that of the Sun. Next, in this figure, there is a rough positive correlation between $r_0(8542)$ and $\langle \text{BVamp} \rangle$. Assuming that the brightness variation of superflare stars is caused by the rotation of a star with starspots, the brightness variation amplitude ($\langle \text{BVamp} \rangle$) corresponds to the starspot coverage of these stars. Then, we can say that there is a rough positive correlation between the starspot coverage and chromospheric activity level ($r_0(8542)$). This rough correlation shows us that all the target stars expected to have large starspots on the basis of their large amplitude of the brightness variation show high magnetic activity compared with the Sun. In other words, our assumption that the amplitude of the brightness variation correspond to the spot coverage is supported, since high magnetic activity, which are confirmed by using $r_0(8542)$ values, are considered to

160 be caused by the existence of large starspots.

161 In Figure 3 (b), we also plot $\langle fB \rangle$ values as a function of $\langle \text{BVamp} \rangle$. $\langle fB \rangle$ values are
 162 estimated from $r_0(8542)$ on the basis of the rough relation estimated in Notsu *et al.*
 163 (2015b) with spectroheliographic observation of a solar active region. With this figure,
 164 we can see the same conclusion as we did with Figure 3 (a), though the errors of $\langle fB \rangle$
 165 values are a bit large especially for less active stars. We also investigated the emission flux
 166 of Ca II IRT and H α lines for reference in Notsu *et al.* (2015b), and confirmed basically
 167 the same conclusions as we did here with $r_0(8542)$ index.

168 4. Summary

169 Superflares are very large flares that release total energy $10\sim 10^4$ times greater than
 170 that of the biggest solar flares ($\sim 10^{32}$ erg). Recent Kepler-space-telescope observations
 171 found more than 1000 superflares on a few hundred solar-type stars. Such superflare stars
 172 show quasi-periodic brightness variations with the typical period of from one to a few
 173 tens of days. Such variations are thought to be caused by the rotation of a star with large
 174 starspots. However, spectroscopic observations are needed in order to confirm whether
 175 the variation is really due to the rotation and whether superflares can occur on ordinary
 176 single stars similar to our Sun.

177 We have carried out spectroscopic observations of 50 solar-type superflare stars with
 178 Subaru/HDS. As a result, more than half (34 stars) of the target stars show no evidence
 179 of the binary system, and we confirmed stellar atmospheric parameters of these stars are
 180 roughly in the range of solar-type stars on the basis of our spectroscopic data.

181 We then conducted the detailed analyses for these 34 stars. First, the value of the $v \sin i$
 182 measured from spectroscopic results is consistent with the rotational velocity estimated
 183 from the brightness variation. Next, we measured the intensity of Ca II IRT and H α
 184 lines, which are good indicators of stellar chromospheric activity. The intensity of these
 185 lines indicates that the mean magnetic field strength ($\langle fB \rangle$) of the target superflare
 186 stars can be higher than that of the Sun. We found a correlation between the amplitude
 187 of the brightness variation and the intensity of Ca II IRT. All the targets expected to
 188 have large starspots because of their large amplitude of the brightness variation show high
 189 chromospheric activity compared with the Sun. These results support that the brightness
 190 variation of superflare stars is explained by the rotation with large starspots.

191 References

- 192 Candelaresi, S., Hillier, A., Maehara, H., *et al.* 2014, *ApJ*, 792, 67
 193 Honda, S., Notsu, Y., Maehara, H., *et al.* 2015, *PASJ*, 67, 85
 194 Koch, D. G., Borucki, W. J., Basri, G., *et al.* 2010, *ApJ*, 713, L79
 195 Maehara, H., Shibayama, T., Notsu, S., *et al.* 2012, *Nature*, 485, 478
 196 Maehara, H., Shibayama, T., Notsu, Y., *et al.* 2015, *Earth, Planets and Space*, 67, 59
 197 Nogami, D., Notsu, Y., Honda, S., *et al.* 2014, *PASJ*, 2014, 66, L4
 198 Noguchi, K., Aoki, W., Kawanomoto, S., *et al.* 2002, *PASJ*, 54, 855
 199 Notsu, S., Honda, S., Notsu, Y., *et al.* 2013a, *PASJ*, 65, 112
 200 Notsu, Y., Shibayama, T., Maehara, H., *et al.* 2013b, *ApJ*, 771, 127
 201 Notsu, Y., Honda, S., Maehara, H., *et al.* 2015a, *PASJ*, 67, 32
 202 Notsu, Y., Honda, S., Maehara, H., *et al.* 2015b, *PASJ*, 67, 33
 203 Schaefer, B. E., King, J. R., & Deliyannis, C. P. 2000, *ApJ*, 529, 1026
 204 Shibata, K. & Magara, T. 2011, *Living Rev. Sol. Phys.*, 8, 6
 205 Shibata, K., Isobe, H., Hillier, A., *et al.* 2013, *PASJ*, 65, 49
 206 Shibayama, T., Maehara, H., Notsu, S., *et al.* 2013, *ApJS*, 209, 5
 207 Takeda, Y., Sato, B., & Murata, D. 2008, *PASJ*, 60, 781
 208 Takeda, Y., Honda, S., Kawanomoto, S., *et al.* 2010, *A&A*, 515, A93